Journal of the Optical Society of America A
OPTICS, IMAGE SCIENCE, AND VISION

Imaging with two skew ideal lenses

JAKUB BĚLÍN* AND JOHANNES COURTIAL

School of Physics & Astronomy, College of Science & Engineering, University of Glasgow, Glasgow G12 8QQ, UK
**Corresponding author: j.belin.1@research.gla.ac.uk*

Received 29 August 2018; revised 12 October 2018; accepted 23 October 2018; posted 26 October 2018 (Doc. ID 344455); published 21 December 2018

In lens systems, the constituent lenses usually share a common optical axis, or at least a common optical-axis direction, and such combinations of lenses are well understood. However, in recent proposals for lens-based transformation-optics devices [Opt. Express 26, 17872 (2018)], the lenses do not share an optical-axis direction. To facilitate the understanding of such lens systems, we describe here combinations of two ideal lenses in any arbitrary arrangement as a single ideal lens. This description has the potential to become an important tool in understanding novel optical instruments enabled by skew-lens combinations.

https://doi.org/10.1364/JOSAA.36.000132

1. INTRODUCTION

Geometrical optics is a mature field, but new ideas keep emerging [1,2]. This applies specifically to the field of lenses: on the one hand, lenses are amongst the oldest optical elements (the Nimrud lens [3] has been dated to between 750 BC and 710 BC) and the basis of a myriad of early optical devices such as spectacles and telescopes; on the other hand, lenses are now being realized in the form of metasurfaces [4–7]. Lenses can also form particularly simple paraxial invisibility cloaks [8]. We have extended the concept of lens-based invisibility cloaks to omni-directional transformation-optics devices [9,10], so far only theoretically. Our transformation-optics devices use very unusual combinations of lenses in which the lenses are at an angle to each other. Note that standard lenses do not work very well when used in such a way, which normally precludes non-paraxial use. However, such non-paraxial lens combinations can be shown to work as desired for specific ray bundles, for example, for one particular viewing position, which should be sufficient to use lens-based transformation-optics devices in a number of applications [10].

For a standard combination of lenses, in which the lenses share an optical axis, it has proved useful and elegant to describe such a system as a single lens with an effective focal length and object- and image-sided principal planes that, in general, do not coincide with each other nor with the principal plane(s) of the individual lenses. This is done by describing object- and image-space positions in special coordinates constructed such that the equations describing the mapping between these spaces have the same form as the standard equations describing the mapping due to a single thin lens.

These special coordinates can be easily constructed from the optical axis and the principal planes of an optical system. However, for combinations of skew lenses, the standard definitions of concepts such as the optical axis lose their meaning; for example, the definition in Ref. [11], "a line through the centers of curvature of the surfaces which make up the optical system," can no longer be applied as the curvature centers in general no longer lie on a (straight) line. The definitions of the cardinal points and cardinal planes (transverse planes through the corresponding cardinal points), including those of the principal planes, such as "If the rays (parallel to the optical axis) entering the system and those emerging from the system are extended until they intersect, the points of intersection will define a surface, usually referred to as the principal plane" [11], need to be scrutinized. Perhaps worse, Fig. 1 shows that a combination of skew lenses exhibits telescope-like behavior, which seems hard to reconcile with a description as a single lens.

We are not aware of a description of combinations of skew lenses as a single lens. In light of the observations in the previous paragraph, this seems unsurprising, but it is actually easy to construct pairs of coordinates—one describing object space, the other describing image space—in which the imaging equations take the form of the ideal-lens mapping; we call coordinates with this property *lens-imaging coordinates*. One way to construct lens-imaging coordinates is to consider the effect of the combination as successive imaging due to the individual lenses but to treat the effect of the first lens as a distortion of object space. Clearly, this is of limited use: it provides no additional insight, and is also mathematically inelegant in the sense that it is non-symmetric (only object space is distorted) and that the distortion is complex enough (parallel lines can be mapped to non-parallel lines, and ratios of distances between points lying on a straight line can change, especially around the focus) to make it hard to gain any intuitive understanding out of the

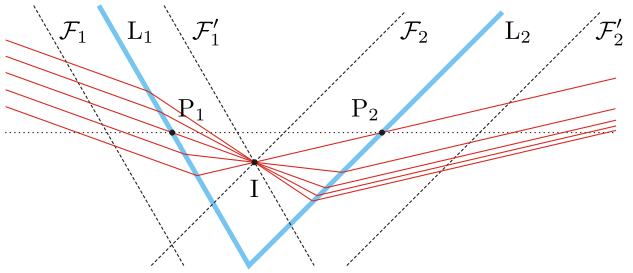

Fig. 1. Telescope-like behavior of a combination of two skew lenses, L_1 and L_2. A bundle of parallel light rays (thin solid lines) is incident on lens L_1 with a direction such that it is focused to a point on the intersection line I between the image-sided focal plane of lens 1, $\mathcal{F}_1'$, and the object-sided focal plane of lens 2, $\mathcal{F}_2$ (dashed lines). Because I lies in the object-sided focal plane of L_2, the bundle is parallel again after transmission through both lenses. The lens planes are shown as thick solid lines; P_1 and P_2 are the principal points of the two lenses.

construction. More interestingly, we can construct lens-imaging coordinates by applying earlier work by Buchroeder on a choice of coordinate systems that simplifies any collinear mapping between object and image space [12]. As ideal lenses map straight lines to straight lines again, the mapping is collinear, that is, it can be written in the form {Eq. (2.1) in Ref. [12]}

$$x' = \frac{a_1 x + b_1 y + c_1 z + d_1}{a_0 x + b_0 y + c_0 z + d_0}, \tag{1}$$

$$y' = \frac{a_2 x + b_2 y + c_2 z + d_2}{a_0 x + b_0 y + c_0 z + d_0}, \tag{2}$$

$$z' = \frac{a_3 x + b_3 y + c_3 z + d_3}{a_0 x + b_0 y + c_0 z + d_0}, \tag{3}$$

where a_i, b_i, c_i, and d_i $(i = 0, \ldots, 3)$ are constants and x, y, z and x', y', z' are the coordinates of the object and image positions, respectively, measured in the same Cartesian coordinate system. If object and image space are described by different Cartesian coordinate systems, which in general have different origins and are rotated relative to each other, this simplifies to {Eq. (2.7) in Ref. [12]}

$$x' = \frac{ax}{z+d}, \qquad y' = \frac{by}{z+d}, \qquad z' = \frac{cz}{z+d}, \tag{4}$$

where a, b, c, and d are constants. We refer to these coordinates as *Buchroeder coordinates*. The anisotropic coordinate scaling $x' \to dx'/a$, $y' \to dy'/b$, $z' \to dz'/c$, which replaces the orthonormal coordinate system in image space with an orthogonal coordinate system, brings the mapping into the form of the ideal-lens mapping,

$$x' = \frac{fx}{z+f}, \qquad y' = \frac{fy}{z+f}, \qquad z' = \frac{fz}{z+f}, \tag{5}$$

where the focal length f is given by the constant d. We call these coordinates *scaled Buchroeder coordinates*.

We describe here an alternative set of lens-imaging coordinates for combinations of two skew lenses. Throughout this paper, we consider ideal thin lenses, for which this construction works perfectly; for real lenses, it works approximately. The starting point for our construction is that the optical axes in object and image space coincide; they are a single straight line. We see this new description as complementary to the scaled Buchroeder coordinates in the sense that different coordinates are better suited for different applications. For example, each is clearly a particularly simple description for imaging of positions on "its" optical axis.

We start by briefly reviewing the standard description of pairs of lenses as a single lens (Section 2). We show the motivation for our construction for single-lens imaging (Section 3) and show, in Section 4, that it works. We then compare the lens-imaging coordinates in Section 5, consider the relevance of our results to physical lenses in Section 6, and discuss several aspects not mentioned elsewhere in Section 7, before concluding (Section 8).

2. REVIEW: IMAGING BY A SINGLE LENS AND BY PAIRS OF COAXIAL LENSES

We start with a brief review of imaging by a single lens and the standard treatment of pairs of coaxial lenses. As always in this paper, "lenses" refers to ideal thin lenses.

A lens has the property that it images stigmatically any point $\mathbf{O} = (x, y, z)^\top$ in object space to a corresponding point $\mathbf{I} = (x', y', z')^\top$ in image space. The coordinate system is chosen such that its origin coincides with the lens's principal point and the z axis coincides with the optical axis. The $z = 0$ plane is the principal plane. If the focal length is f, the object and image positions are related by the equations

$$-\frac{1}{z} + \frac{1}{z'} = \frac{1}{f} \tag{6}$$

and

$$\frac{x'}{x} = \frac{y'}{y} = \frac{z'}{z}. \tag{7}$$

It can easily be shown that these equations are equivalent to the equations describing the mapping between object and image space in scaled Buchroeder coordinates, Eq. (5).

Pairs of coaxial lenses, L_1 and L_2 (Fig. 2), can be described as a single lens whose object- and image-sided principal planes no longer coincide ([11], Chap. 2.10). The effective focal length, f, can be found using the Gullstrand equation ([11], Chap. 2.10)

$$f = \frac{f_1 f_2}{f_1 + f_2 - d}, \tag{8}$$

where f_1 and f_2 are the focal lengths of the lenses. If we place a Cartesian coordinate system such that its origin lies at P_1 and the optical axis coincides with the common optical axis, then the z coordinates of the principal points of the combined system, P and P′, are given by the equations

$$P_z = \frac{df}{f_2}, \qquad P_{z'} = d - \frac{df}{f_1}. \tag{9}$$

The image position (x', y', z') of any point (x, y, z) due to the two-lens system can then be found using the equations

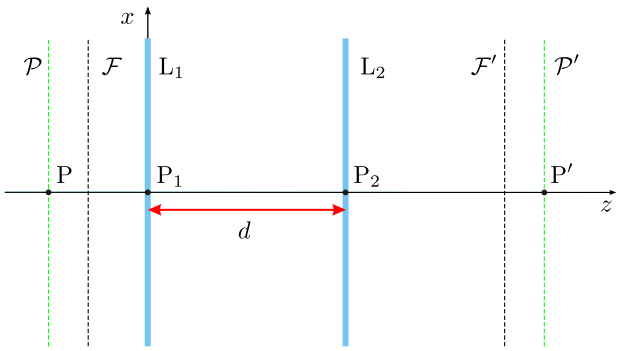

Fig. 2. Geometry of a system of two coaxial lenses, L_1 and L_2, separated by a distance d. The optical axes of the individual lenses coincide with the z axis. The focal planes, $\mathcal{F}$ and $\mathcal{F}'$, and the principal planes, $\mathcal{P}$ and $\mathcal{P}'$, of the combined system are shown as dashed lines.

$$-\frac{1}{z-P_z}+\frac{1}{z'-P_{z'}}=\frac{1}{f}, \tag{10}$$

$$\frac{x'}{x}=\frac{y'}{y}=\frac{z'-P_{z'}}{z-P_z}. \tag{11}$$

If we shift the origin of the object-space coordinate system to coincide with P and the origin of the image-space coordinate system to coincide with P′, i.e., by making the substitutions $z - P_z \to z$ and $z' - P_{z'} \to z'$, this set of equations takes the form of the standard thin-lens imaging equations, Eqs. (6) and (7).

3. MOTIVATION FOR LENS-IMAGING COORDINATES

We want to describe the effect of two lenses as that of a single lens in suitable coordinates. We want symmetric and affine coordinates (which preserve parallel lines and distance ratios between points on a straight line) in which the imaging equations have the standard form. We will have to generalize concepts, e.g., the optical axis of the two-lens system will no longer coincide with the axis of symmetry of the system (because there is none).

A. Lens-Imaging Coordinates for a Single Lens

We start by applying a generalized concept of an optical axis to the particularly simple example of a single lens.

The equations describing the thin-lens mapping, Eqs. (6) and (7), are written in Cartesian (x, y, z) coordinates, chosen such that the lens is in the $z = 0$ plane, its principal point, P, coincides with the origin, and the z axis is the optical axis. We can also describe the mapping in a skew coordinate system with coordinates u, v, and w, whose origin is again at P, whose u and v axes coincide with the x and y axes, and whose w axis is at an angle α with the z axis in the (x, z) plane (Fig. 3).

We consider a pair of conjugate points, $\mathbf{O} = u\hat{\mathbf{u}} + v\hat{\mathbf{v}} + w\hat{\mathbf{w}}$ and $\mathbf{I} = u'\hat{\mathbf{u}} + v'\hat{\mathbf{v}} + w'\hat{\mathbf{w}}$. As $z = w\cos\alpha$, and with the crucial definition of the *projected focal length*

$$g=\frac{f}{\cos\alpha}, \tag{12}$$

En. (6) becomes

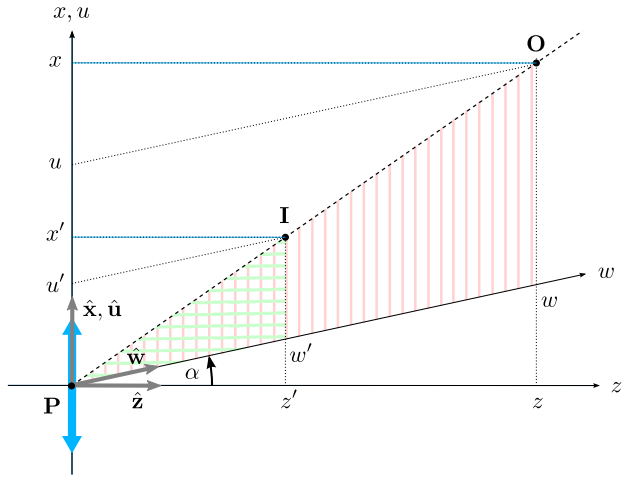

Fig. 3. Coordinates for single-lens imaging. A pair of conjugate positions, **O** and **I**, is shown. In a Cartesian (x, y, z) coordinate system, placed such that the lens is in the $z = 0$ plane and the position of the principal point, **P**, coincides with the origin, the relationships between the coordinates of **O** and **I** have the standard form, given by Eqs. (6) and (7). The object and image positions can alternatively be expressed in skew coordinates with basis vectors $\hat{\mathbf{u}}$, $\hat{\mathbf{v}}$, and $\hat{\mathbf{w}}$, with the imaging equations retaining their standard form. The figure shows a cross section in the $y = v = 0$ plane.

$$-\frac{1}{w}+\frac{1}{w'}=\frac{1}{g} \tag{13}$$

and therefore remains of the standard form [Eq. (6)]. Because of the similarity of the triangles highlighted in Fig. 3, Eq. (7) becomes

$$\frac{u'}{u}=\frac{v'}{v}=\frac{w'}{w} \tag{14}$$

and also retains the relevant standard form [Eq. (7)]. In this sense, any choice of the w axis, provided it passes through the principal point at $w = 0$, is therefore a perfectly good choice of optical axis.

B. Optical Axis of a Two-Lens System

A straight line through the principal points of L_1 and L_2 has the property that the combination images it back to the same line, and we just worked out that this line is a perfectly good optical axis for each lens individually. It is therefore an excellent candidate for the optical axis of the combination.

Once the optical axis is defined, we can describe the imaging properties of the two-lens system for an object lying on this axis. As above, we define w to be the coordinate along the optical axis, and for the moment we choose its origin to coincide with P_1. According to Eq. (12), the projected focal lengths of the two lenses are

$$g_1=\frac{f_1}{\cos\varphi_1}, \qquad g_2=\frac{f_2}{\cos\varphi_2}, \tag{15}$$

where φ_1 and φ_2 are the angles between the two-lens optical axis and the optical axes of the individual lenses (see Fig. 4). As a system of two lenses can be effectively understood as a single thick lens, we can calculate the effective focal length f,

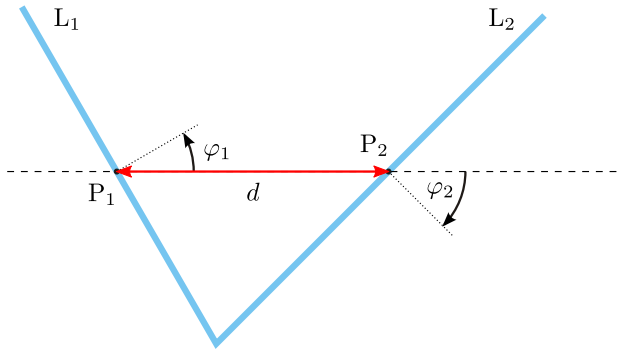

Fig. 4. General system of two lenses L_1 and L_2 (thick cyan lines). Our choice of optical axis for this two-lens system, the two-lens optical axis (dashed line), passes through both principal points P_1 and P_2. ϕ_1 and ϕ_2 are the angles between the lens normals and the two-lens optical axis.

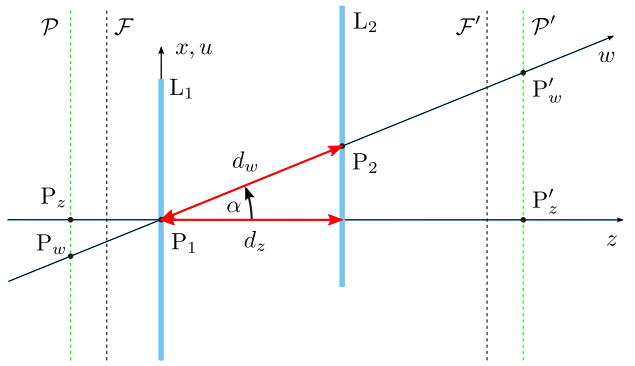

Fig. 5. System of two parallel but non-coaxial lenses. The red dashed lines correspond to the focal lines of this system and the green dashed lines correspond to its principal lines with principal points P and P′. It is clear that point P′ is imaged to a point P′ by this optical device.

the *two-lens focal length*, using the Gullstrand equation, Eq. (8),

$$f = \frac{g_1 g_2}{g_1 + g_2 - d}, \tag{16}$$

and use the standard thick-lens theory to calculate the values P_w and $P_{w'}$ of the w coordinate of the object and image-sided two-lens principal points, P and P′, as

$$P_w = \frac{df}{g_2}, \tag{17}$$

$$P_{w'} = d - \frac{df}{g_1}. \tag{18}$$

The image position w' for any object position w lying on the optical axis can be then found using the equation

$$-\frac{1}{w - P_w} + \frac{1}{w' - P_{w'}} = \frac{1}{f}. \tag{19}$$

Encouragingly, this is of the same form as the axial-imaging equation for pairs of coaxial lenses, Eq. (10). So far, our choice of optical axis therefore appears to be a good choice.

C. Example: Parallel Non-Coaxial Lenses

So far, we have a candidate for the optical axis, which would be the w axis. At this stage, it is instructive to try to complete the set of lens-imaging coordinates for a simple but non-trivial example: a generalization of the coaxial two-lens system from Section 2 in which the lenses are shifted relative to each other in the x direction (Fig. 5).

We make the following choices for the coordinate system. The w coordinate is along the optical axis through the principal points P_1 and P_2. The transverse coordinates, u and v, are chosen to be parallel to x and y, respectively. The coordinate transformation from u, v, and w to x, y, and z is then

$$u = x - z\tan\alpha, \qquad v = y, \qquad w = \frac{z}{\cos\alpha}. \tag{20}$$

If u, v, and w are indeed lens-imaging coordinates, then the mapping between object and image space is of the standard form given by Eqs. (6) and (7),

$$-\frac{1}{w - P_w} + \frac{1}{w' - P_{w'}} = \frac{1}{F}, \qquad \frac{u'}{u} = \frac{v'}{v} = \frac{w' - P_{w'}}{w - P_w}, \tag{21}$$

where $P_w = P_z/\cos\alpha$, $P_{w'} = P_{z'}/\cos\alpha$ [P_z and $P_{z'}$ are given by Eq. (9)], and $F = f/\cos\alpha$, where f is given by the Gullstrand equation [Eq. (8)]. To express these equations in the Cartesian coordinates, the transformation from Eq. (20) can be employed. After simplifying the results and inserting the above expressions for the parameters P_w, $P_{w'}$, and F, we obtain

$$-\frac{1}{z - P_z} + \frac{1}{z' - P_{z'}} = \frac{1}{f}, \qquad \frac{x' - P_{z'}\tan\alpha}{x - P_z\tan\alpha} = \frac{y'}{y} = \frac{z' - P_{z'}}{z - P_z}. \tag{22}$$

It can be seen that the effect of the transverse displacement of L_2 on the image is simply a transverse shift of the image in the direction of the displacement (here x), given by $(P_{z'} - P_z)\tan\alpha$. Note that these equations can be brought into the standard form of Eqs. (6) and (7), provided the origins of the coordinate systems in object and image space are shifted such that $(x, y, z) \to (x - P_z\tan\alpha, y, z - P_z)$ and $(x', y', z') \to (x' - P_{z'}\tan\alpha, y', z' - P_{z'})$. Therefore, the coordinates $(x - P_z\tan\alpha, y, z - P_z)$ and $(x' - P_{z'}\tan\alpha, y', z' - P_{z'})$ are also lens-imaging coordinates. In fact, it can be shown that they are the scaled Buchroeder coordinates for this combination.

Successive imaging by the individual lenses results in the same mapping, as we show in Code 1, Ref. [13] (TwoParallelLensProof.nb). It is encouraging to see that, in this simple example, our choice of optical axis (and w axis) can be completed into lens-imaging coordinates. The other two coordinates point in the transverse directions, but what are these in the general case?

D. Transverse Planes

In the examples studied above, transverse planes had a number of properties. One very special property is that the transverse planes in object space form a set of parallel planes, which has the property that it is imaged to another set of parallel planes, namely, the image-space transverse planes. Therefore, we attempt to find two

sets of parallel planes, one in object space and the other in image space, that are imaged into each other.

To find such conjugated sets of parallel planes, we use (maybe surprisingly) the mysterious telescope-like property, which at first does not seem to have an analogue in the case of a lens. Figure 1 shows that the telescope-like behavior can be observed if a bundle of parallel light rays is incident on lens L_1 with a direction such that it is focused to a point lying on the intersection line I between the image-sided focal plane $\mathcal{F}_1'$ of lens L_1 and the object-sided focal plane $\mathcal{F}_2$ of lens L_2. Since line I lies in the object-sided focal plane of lens L_2, the ray bundle focused on I becomes parallel again after emerging the lens L_2.

For the moment, let us consider one subset of these "telescope rays," intersecting at an arbitrary point in object space. The object-space parts of those rays, that is, the part of the rays before they intersect L_1, form a plane parallel to the one through P_1 and line I; the image-space parts form a plane parallel to the plane through line I and principal point P_2. It is clear that any point lying in the object-space plane is then imaged to a point lying in the image-space plane. If the subset of telescope rays intersecting at a point outside this plane is considered, a different pair of conjugate planes, the object-sided planes parallel to each other and the image-space planes as well, is formed. The set of all such object-space planes and the set of the corresponding image-space planes then form two sets of parallel planes that are imaged into each other. The planes constructed in this way satisfy our requirements for transverse planes, and therefore we will refer to them as object- and image-sided skew-lens transverse planes.

In the case of parallel lenses L_1 and L_2, our construction of the transverse planes results in the standard transverse planes parallel to the lens planes. (Line I then lies at an infinite distance from the optical axis.)

E. Focal Planes

In this section, we will find the focal planes of the two-lens system and show that these planes satisfy our definition of skew-lens transverse planes. Since focal planes are well defined, we can simply use the standard definitions, such as [14] "Rays which are parallel in the object space will be transformed into rays which intersect in a point on the [image-space] focal plane […]. Similarly rays from a point in the [object-space] focal plane […] will transform into a pencil of parallel rays." The focal points are, of course, the intersections of those planes with the optical axis.

Following the above definitions, we construct the focal planes as follows. Figure 6(a) shows parallel rays incident on the lens combination from object space. Lens L_1 redirects the light rays such that they intersect in a point in the image-sided focal plane of L_1. Note that this intersection point can be real (as shown in Fig. 6) or virtual. This point is then re-imaged by lens L_2, and so, after transmission through both lenses, the rays intersect in this final image point, which therefore lies in the image-sided focal plane of the lens combination. This two-lens image-sided focal plane is therefore the image, due to lens L_2, of the image-sided focal plane of lens L_1. As the lenses are, in general, skew, the image-sided focal plane of L_1 intersects the plane of L_2 in a line, I_2. As I_2 lies in the image-sided focal plane of L_1,

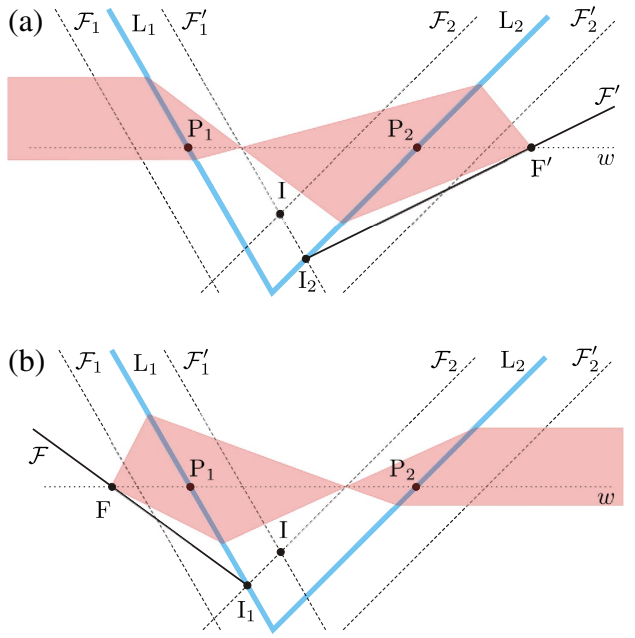

Fig. 6. Construction of the (a) image-sided and (b) object-sided two-lens focal planes, $\mathcal{F}'$ and $\mathcal{F}$. The image-sided two-lens focal plane, $\mathcal{F}'$, is the image due to L_2 of the image-sided focal plane $\mathcal{F}_{1'}$ of lens L_1. Similarly, $\mathcal{F}$ is imaged by L_1 to the object-sided focal plane $\mathcal{F}_2$ of L_2. The image- and object-sided focal points, F′ and F, are the intersections of the corresponding focal planes with the optical axis.

its image due to L_2 lies in the two-lens image-sided focal plane, but as I_2 also lies in the plane of L_2, L_2 simply images I_2 to itself. I_2 therefore lies in the two-lens image-sided focal plane.

However, the image-sided focal plane $\mathcal{F}_1'$ of lens L_1 also passes through line I. Therefore, its image due to lens L_2—the two-lens image-sided focal plane—is an image-sided transverse plane according to the construction in Section 3.D. Reassuringly, we have thus confirmed that the two-lens image-sided focal plane $\mathcal{F}'$ is an image-sided transverse plane.

Similarly, we can construct the two-lens object-sided focal plane, $\mathcal{F}$. Lens L_1 images $\mathcal{F}$ into $\mathcal{F}_2$, the object-sided focal plane of lens L_2. $\mathcal{F}$ therefore intersects L_1 in the same line I_1 as the object-sided focal plane of lens L_2. Again, the object-sided focal plane $\mathcal{F}_2$ of lens L_2 passes through line I, and therefore it is an image of an object-sided transverse plane due to lens L_1. The object-sided two-lens focal plane $\mathcal{F}$ is therefore an object-sided transverse plane.

In Section 3.B we already calculated the two-lens focal length, f, and the w coordinates of the two-lens principal points, P_w and $P_{w'}$. From these, we can easily calculate the w coordinates of the focal points to be

$$F_w = P_w - f, \tag{23}$$

$$F_{w'} = P_w' + f. \tag{24}$$

Now we will prove that these are the intersections of our two-lens focal planes with the optical axis. Figure 6(b) indicates that the intersection F_w of the object-sided focal plane satisfies the imaging equation

$$-\frac{1}{F_w}+\frac{1}{d-g_2}=\frac{1}{g_1}, \tag{25}$$

and so

$$F_w=\frac{g_1 d-g_1 g_2}{g_1+g_2-d}. \tag{26}$$

Expressing this in terms of the two-lens focal length f, defined in Eq. (16), and the w coordinate of the object-sided two-lens principal point, P_w, we obtain Eq. (23).

Similarly, using Fig. 6(a), we can deduce that

$$F'_w=d+\frac{g_1 g_2-g_2 d}{g_1+g_2-d}. \tag{27}$$

Expressed in terms of f and P'_w, this yields Eq. (24). Everything is consistent so far.

F. Principal Planes

We start from the following definition of principal planes [11]: "If the rays (parallel to the optical axis) entering the system and those emerging from the system are extended until they intersect, the points of intersection will define a surface, usually referred to as the principal plane." It is possible to find a set of points that satisfy this definition immediately: the intersection line V of the planes of lenses L_1 and L_2 (Fig. 7). This line is imaged back to itself by the two-lens system, i.e., any light ray hitting the two-lens system at V emerges again from V and therefore at the same distance from the optical axis, so line V is a sensible candidate for the intersection of the principal planes of the two-lens system.

With this choice, the object-sided two-lens principal plane $\mathcal{P}$ is then the object-sided transverse plane passing through line V, and the image-sided two-lens principal plane $\mathcal{P}'$ is the image-sided transverse plane through V. The corresponding principal points, P and P′, are then the intersections of the corresponding two-lens principal planes with the optical axis. Figure 7 shows this construction.

To find the intersections of our principal planes with the optical axis, we will use the fact that the intermediate image of the object-sided principal plane $\mathcal{P}$ due to lens L_1 lies in a plane through both lines V (as each lens images V to itself) and I (as $\mathcal{P}$ and $\mathcal{P}'$ are transverse planes; see Fig. 7). In fact, it is possible to show that such a plane intersects the optical axis at w value

$$w_{\mathrm{im}}=\frac{d g_1}{g_1+g_2}. \tag{28}$$

The w coordinate of the object-sided principal point, P_w, then satisfies the imaging equation

$$-\frac{1}{P_w}+\frac{1}{w_{\mathrm{im}}}=\frac{1}{g_1} \tag{29}$$

or, solved for P_w and writing the result in terms of the two-lens focal length f [Eq. (16)],

$$P_w=\frac{d f}{g_2}, \tag{30}$$

which is the same as Eq. (17), the result we obtained earlier from our considerations of axial imaging.

Analogously, the w coordinate of the image-sided principal point, $P_{w'}$, has to satisfy the equation

$$-\frac{1}{w_{\mathrm{im}}-d}+\frac{1}{P_{w'}-d}=\frac{1}{g_2}, \tag{31}$$

which again confirms the earlier axial-imaging result, in this case Eq. (18).

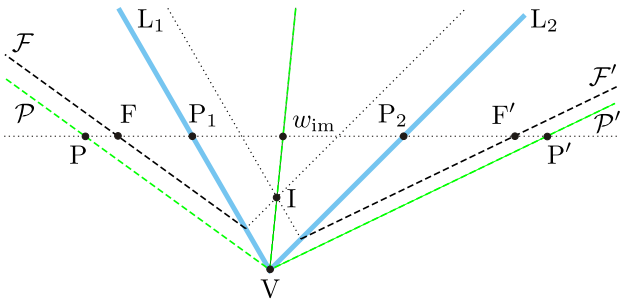

Fig. 7. Construction of the two-lens object- and image-sided principal planes, $\mathcal{P}$ and $\mathcal{P}'$. $\mathcal{P}$ is the object-sided transverse plane through V, the line where the lens planes intersect; $\mathcal{P}'$ is the image-sided transverse plane through V. The corresponding principal points P and P′ are the intersections of $\mathcal{P}$ and $\mathcal{P}'$ with the optical axis. The intermediate image of the object-sided principal plane $\mathcal{P}$ due to lens L_1 is the plane through both lines V and I. It intersects the optical axis at point w_{im}.

4. LENS-IMAGING COORDINATES IN ACTION!

Now we are ready to define the two-lens lens-imaging coordinates. We describe positions in object space using a skew, non-normalized (u, v, w) coordinate system with its origin at P. The w axis coincides with the two-lens optical axis, but note that the origin is no longer at P_1, as in the previous sections, but at P. The u and v axes lie in the object-sided principal plane, $\mathcal{P}$. Similarly, image-space positions are expressed in the skew, non-normalized (u', v', w') coordinate system with its origin at P′.

A. Two-Dimensional (2D) Case

We start with a two-lens system in two dimensions. Transverse planes are then transverse lines, and the intersection lines I and V are intersection points.

Figure 8 shows the geometry of this setup, together with a set of basis vectors that defines object- and image-sided lens-imaging coordinates. The object-sided lens-imaging basis consists of a unit vector, $\hat{\mathbf{w}}$, parallel to the optical axis and a (non-unit) vector, $\mathbf{u}$, parallel to the object-sided transverse lines and with its length chosen such that its component perpendicular to $\hat{\mathbf{w}}$ is of magnitude 1. The origin of the $(\mathbf{u}, \hat{\mathbf{w}})$ coordinate system is the object-sided principal point, P. Similarly, the image-sided lens-imaging basis consists of a unit vector, $\hat{\mathbf{w}}'$, that is again parallel to the optical axis, and a (non-unit) vector $\mathbf{u}'$ parallel to the image-sided transverse lines and with a component perpendicular to $\hat{\mathbf{w}}'$ of magnitude 1, and the origin lies at the image-sided principal point, P′.

We are now assuming that the (u, w) and (u', w') coordinates are object- and image-sided lens-imaging coordinates, which means that the imaging equations that map an object position (u, w) to a corresponding image position (u', w') are of the standard form [Eq. (5)]

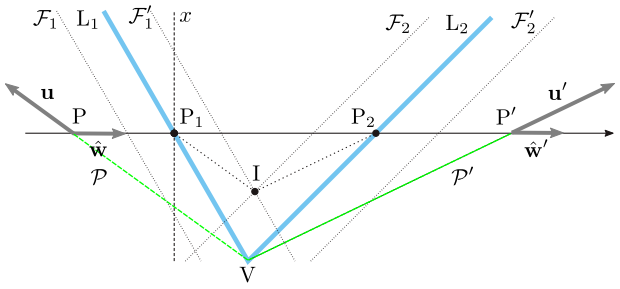

Fig. 8. Geometry of a system of two 2D skew lenses, and definition of the two-lens lens-imaging coordinates. The lens-imaging basis is given by vectors $\mathbf{u}$ and $\hat{\mathbf{w}}$ in object space and $\mathbf{u}'$ and $\hat{\mathbf{w}}'$ in image space. The origins of the lens-imaging coordinates coincide with two-lens principal points P and P′, respectively. For the purposes of calculations, a Cartesian coordinate system (x, z) has been chosen such that z-axis coincides with the generalized optical axis of the two-lens system (i.e., a line passing through both principal points P_1 and P_2 of the individual lenses) and the origin coincides with principal point P_1 of lens L_1.

$$\begin{pmatrix} u' \\ w' \end{pmatrix} = \frac{f}{w+f} \begin{pmatrix} u \\ w \end{pmatrix}, \tag{32}$$

where f is the effective focal length defined by Eq. (16). To show that our assumption is correct, we prove that successive imaging by L_1 and L_2 gives the same mapping as that in Eq. (32).

First, we transform Eq. (32) from lens-imaging coordinates into Cartesian coordinates (in which the calculation of successive imaging due to L_1 and L_2 is easy), specifically the Cartesian coordinates (x, z) defined in Fig. 8. In these coordinates, the transverse lines with axial coordinate w (in object space) and w' (in image space) are given by the equations

$$x = k_o(z - P_z - w) \qquad \text{object space}, \tag{33}$$

$$x' = k_i(z' - P_{z'} - w') \qquad \text{image space}, \tag{34}$$

where k_o and k_i are the slopes of the transverse lines in object and image space, respectively, and these are given by the equations

$$k_o := \frac{x_I}{z_I} = -\cot\varphi_1 \frac{d - g_1 - g_2}{d - g_2 - g_1(\cot\varphi_1/\cot\varphi_2)}, \tag{35}$$

$$k_i := \frac{x_I}{z_I - d} = -\cot\varphi_2 \frac{d - g_1 - g_2}{d - g_1 - g_2(\cot\varphi_2/\cot\varphi_1)}, \tag{36}$$

where x_I and z_I are the Cartesian coordinates of point I. Because of our choice of the length of the basis vectors $\mathbf{u}$ and $\mathbf{u}'$,

$$x = u, \qquad x' = u'. \tag{37}$$

In fact, Eqs. (33) and (37) provide a coordinate transformation $(x, z) \to (u, w)$ in object space if one solves for the variables u and w, resulting in the expressions

$$w = z - P_z - \frac{x}{k_o}, \qquad u = x. \tag{38}$$

In matrix representation,

$$\begin{pmatrix} u \\ w \end{pmatrix} = \begin{pmatrix} 1 & 0 \\ -\frac{1}{k_o} & 1 \end{pmatrix} \begin{pmatrix} x \\ z - P_z \end{pmatrix}. \tag{39}$$

Similarly, the image-space transformation $(u', w') \to (x', z')$ is

$$\begin{pmatrix} x' \\ z' - P_z' \end{pmatrix} = \begin{pmatrix} 1 & 0 \\ \frac{1}{k_i} & 1 \end{pmatrix} \begin{pmatrix} u' \\ w' \end{pmatrix}. \tag{40}$$

Doing these coordinate transformations and using the definitions fixed above, the Cartesian coordinates of the image position can be found to be

$$x' = \frac{fx}{f + z - \frac{x}{k_o} - P_z}, \tag{41}$$

$$z' = P_{z'} + \frac{f(z - x\frac{k_i - k_o}{k_i k_o} - P_z)}{f + z - \frac{x}{k_o} - P_z}. \tag{42}$$

In vector form, the mapping between object and image space due to a single lens with its principal point at $\mathbf{P}$, optical-axis direction $\hat{\mathbf{n}}$ (chosen to point in the direction from object space to image space), and focal length f can be written in the form

$$\mathbf{I} - \mathbf{P} = \frac{f}{f + (\mathbf{O} - \mathbf{P}) \cdot \hat{\mathbf{n}}} (\mathbf{O} - \mathbf{P}), \tag{43}$$

which is easily derived from Eq. (3) in Ref. [15]. Using this equation, and in the Cartesian coordinates (x, z) defined in Fig. 8, we calculated the image due to the two lenses of an object at position (x, z). This calculation was performed in Code 1, Ref. [13] (TwoLensProof2D.nb), yielding the same results. In 2D, our concept of lens-imaging coordinates therefore works for a general system of two skew lenses.

B. Three-Dimensional (3D) Case

The basis vectors for our 3D lens-imaging coordinates, u, v, and w in object space and u', v', and w' in image space, are defined in Fig. 9. Like in the 2D case, the lengths of $\mathbf{u}$ and $\mathbf{u}'$ are chosen such that their components perpendicular to the optical axis are 1. Therefore, $\mathbf{u}$ and $\mathbf{u}'$ are not normalized, but all other basis vectors are.

We want to apply an argument analogous to that we used in the 2D case. We start with the standard imaging equation, i.e., Eq. (5), which can again be written in vector form [the equivalent of Eq. (32)] in 3D. As in the 2D case, we transform this into Cartesian coordinates, x, y, and z, chosen as follows: the y axis is parallel to the line V, the x direction is given by the cross product $\hat{\mathbf{y}} \times \hat{\mathbf{w}}$, and the unit vector in the z direction is $\hat{\mathbf{z}} = \hat{\mathbf{x}} \times \hat{\mathbf{y}}$. The origin of this system lies at the principal point P_1, i.e., the principal point of lens L_1.

Like in the 2D case, we want to formulate this in matrix form, so we need to find the equivalent of the matrix in Eq. (40). This matrix, which we call T_i^{-1} and which describes the image-space transformation $(u', v', w') \to (x', y', z')$, can be deduced from Fig. 9 to be

$$T_i^{-1} = \begin{pmatrix} 1 & 0 & 0 \\ \frac{\tan\alpha}{k_i} & 1 & \sin\alpha \\ \frac{1}{k_i} & 0 & \cos\alpha \end{pmatrix}, \tag{44}$$

where α is the angle between the w and z axes. The matrix describing the object-space transformation

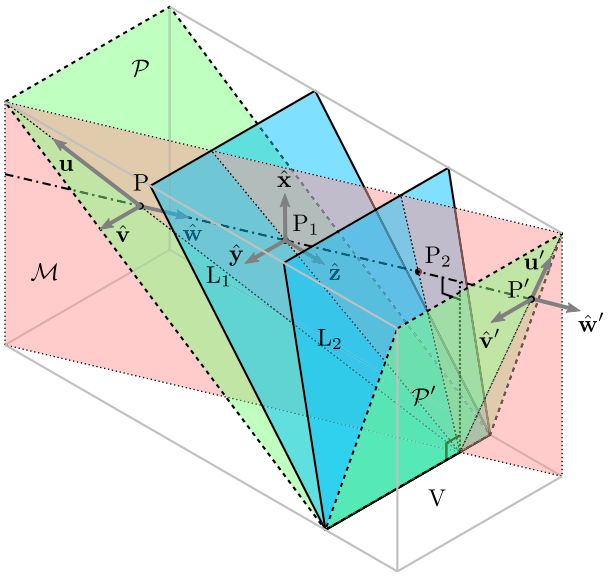

Fig. 9. Definition of the object- and image-space lens-imaging coordinates in three dimensions. Object and image space are described in terms of skew coordinate systems with basis vectors $\mathbf{u}$, $\hat{\mathbf{v}}$, $\hat{\mathbf{w}}$ (object space) and $\mathbf{u}'$, $\hat{\mathbf{v}}'$, $\hat{\mathbf{w}}'$ (image space). Note that the basis vectors in the u and u' directions are not normalized. $\mathbf{u}$ lies on the intersection of the object-sided principal plane, $\mathcal{P}$, and the median plane, $\mathcal{M}$; $\mathbf{u}'$ lies on the intersection of the image-sided principal plane, $\mathcal{P}'$, and the median plane, $\mathcal{M}$. P and P′ are the object- and image-sided principal points.

$(x, y, z) \to (u, v, w)$ is then the inverse of T_i^{-1} with the image-space slope k_i replaced by the object-space slope k_o, which can be expressed in the form

$$T_o = \begin{pmatrix} 1 & 0 & 0 \\ 0 & 1 & -\tan\alpha \\ 0 & -\frac{1}{k_o \cos\alpha} & \frac{1}{\cos\alpha} \end{pmatrix}. \tag{45}$$

The equivalent of Eq. (40), that is, the imaging equation derived from the 3D standard imaging equation in lens-imaging coordinates, can then be written in the form

$$\mathbf{I} - \mathbf{P}' = T_i^{-1} \begin{pmatrix} u' \\ v' \\ w' \end{pmatrix} = \frac{f}{w+f} T_i^{-1} T_o (\mathbf{O} - \mathbf{P}), \tag{46}$$

which is a generalization of the imaging equation derived in Ref. [15] when the imaging system contains two principal points with position vectors $\mathbf{P}$ and $\mathbf{P}'$. Written explicitly, this imaging equation becomes

$$\begin{pmatrix} x' \\ y' - P_{z'} \sin\alpha \\ z' - P_{z'} \cos\alpha \end{pmatrix} = \frac{f}{w+f} \begin{pmatrix} 1 & 0 & 0 \\ \frac{k_o - k_i}{k_i k_o} \tan\alpha & 1 & 0 \\ \frac{k_o - k_i}{k_i k_o} & 0 & 1 \end{pmatrix} \begin{pmatrix} x \\ y - P_z \sin\alpha \\ z - P_z \cos\alpha \end{pmatrix}. \tag{47}$$

We compared this result to that due to successive application of the equations describing imaging due to the individual lenses. We performed this calculation in Code 1, Ref. [13] (TwoLensProof.nb), finding that the resulting image positions are identical. Our choice of lens-imaging coordinates therefore works.

5. COMPARISON OF LENS-IMAGING COORDINATE SYSTEMS

It is instructive to compare the two lens-imaging coordinate systems defined here, namely the scaled Buchroeder coordinates [see Eq. (5)] and the coordinates defined in Section 4. The former uses two Cartesian coordinate systems, i.e., two ortho*normal* coordinate systems), the latter use two affine (skew, non-normalized) coordinate systems. Without detailed proofs, we state here similarities and differences of these two sets of coordinate systems.

It is clear that the focal planes must be the same, as these have a very specific physical meaning. The two descriptions also agree in their definition of the transverse planes (called "normal planes" in Ref. [12]), as these are the only sets of parallel planes in object and image space that are imaged into each other. The principal planes are also the same.

The descriptions differ in their choice of optical axis and therefore also in the positions of the cardinal points, which lie at the intersections between the optical axis and the focal planes and principal planes. In our description, the optical axis is the straight line through the principal points of the two lenses, whereas in the Buchroeder description, the optical axis is defined by the trajectory of the one light ray that is perpendicular to the transverse planes both in object and in image space. The optical axes in object and image space therefore coincide in our description (but their origins differ), whereas the Buchroeder optical axes in object and image space do not lie on the same straight line and are in general not even parallel. The two choices for the optical axis are identical if and only if the two lenses share the same (standard) optical axis.

To derive the precise relationship between the coordinates, we express the unscaled Buchroeder coordinates [Eq. (4)] in terms of our affine coordinates. We do this for the simpler 2D case. The relevant Buchroeder equations are

$$x' = \frac{ax}{z+d}, \qquad z' = \frac{cz}{z+d}. \tag{48}$$

The connections between the coordinates (x, z) and (u, w) and between (x', z') and (u', w') are

$$\begin{aligned} x &= \frac{u - u_P}{\cos\theta} - w \sin\theta, \\ z &= w \cos\theta, \\ x' &= \frac{u' - u'_{P'}}{\cos\theta'} - w' \sin\theta', \\ z' &= w' \cos\theta', \end{aligned} \tag{49}$$

where

$$u_P = u'_{P'} = f\left(\frac{1}{k_i + 1/k_i} - \frac{1}{k_o + 1/k_o}\right) \tag{50}$$

is the value of the u and u' coordinates of the Buchroeder principal points, θ is the angle between the w and z axes, and θ' is the angle between the w' and z' axes. Inserting these expressions into the equation for the standard lens mapping, Eq. (32), expressing the trigonometric functions of θ in terms of k_o and k_i, e.g.,

Table 1. Comparison between Scaled Buchroeder Coordinates and the Lens-Imaging Coordinates Introduced Here[a]

	Skew Lenses	Parallel Non-Coaxial Lenses	Parallel Coaxial Lenses
Optical axis	Different	Different	Same
Transverse planes	Same	Same	Same
Focal planes	Same	Same	Same
Principal planes	Same	Same	Same
Focal points	Different	Different	Same
Principal points	Different	Same	Same
Focal length	Different	Different	Same

[a]The three columns refer to different two-lens configurations; the rows list different entities.

$$\tan\theta = \frac{1}{k_o}, \qquad \tan\theta' = \frac{1}{k_i}, \tag{51}$$

and comparing with the set of equations Eqs. (49) leads to the following relations:

$$a = f\frac{\sqrt{1+\frac{1}{k_i^2}}}{1+\frac{1}{k_o^2}}, \tag{52}$$

$$c = \frac{f}{\sqrt{1+\frac{1}{k_i^2}}}, \tag{53}$$

$$d = \frac{f}{\sqrt{1+\frac{1}{k_o^2}}}. \tag{54}$$

We make a number of observations.

1. If $k_i = k_o$, then $u_P = u'_{P'} = 0$, and so the origins of the (u, w) and (x, z) coordinate systems describing object space coincide, as do the origins of the coordinate systems describing image space. These origins are, of course, the principal points, so they are different in general, but the same if the principal planes in object and image space are parallel, which in turn is the case if either the two lenses are parallel, or if the principal points of both lenses coincide and lie on V.
2. If $|k_o| = |k_i|$, then $a = c = d$, and so the scaling factors between the (unscaled) Buchroeder coordinates and the scaled Buchroeder coordinates are all 1, which in turn means that the scaled Buchroeder coordinates are the same as the (unscaled) Buchroeder coordinates. Substitution into the mapping formulated in terms of the unscaled Buchroeder coordinates, Eq. (48), and comparing the resulting equations to the mappings in terms of the scaled Buchroeder coordinates, Eq. (5), reveals that a, c, and d have the meaning of the (Buchroeder) focal length, which is different from the effective focal length in our coordinates as the optical axes are not parallel.

Table 1 summarizes the similarities and differences between the different lens-imaging coordinates.

6. COMBINATIONS OF SKEW PHYSICAL LENSES

So far, we have assumed ideal thin lenses in our construction. Do our results also apply to physical lenses?

Conventional physical lenses are designed to image in the paraxial regime and suffer from many imperfections, for example, barrel distortion, which alters the mapping between object and image space, and coma, which degrades the quality of non-paraxial images. In the case of our combinations of two skew lenses, at least one of the lenses is used non-paraxially. For this reason, combinations of skew conventional lenses do not image well, which is possibly the reason why such combinations are used only rarely (one example of their use can be found in Ref. [16]) and, to the best of our knowledge, our description of combinations of skew lenses is new.

However, lenses (or indeed, lens holograms) can be optimized to image non-paraxially. This imaging can even be stigmatic (i.e., ray-optically perfect), but in the case of a thin lens hologram this is possible only for a single pair of conjugate positions, and in the case of lenses comprising two surfaces for two pairs of conjugate positions [17]. This is sufficient to enable applications in which either point light sources or point-like observers are located in these positions.

A relevant recent development is the emergence of metalenses [4–7]: metasurface phase holograms [18–23] with properties that aim to approximate those of ideal thin lenses. The metasurface properties can be tuned in many ways; this has, for example, enabled the development of low-dispersion metalenses [7,24,25]. The field of metalenses is currently progressing rapidly and is expected to lead to closer approximations of ideal thin lenses with reduced aberrations such as coma [26]. Our construction has the potential to become a useful tool for the description of such metalenses.

7. DISCUSSION

It is well known that two parallel lenses become telescopic in the confocal case, namely, when the image-sided focal plane of the first lens coincides with the object-sided focal plane of the second lens. For such a combination, the effective focal length and the distance of the principal planes from the lenses become infinite, which means the description in terms of lens-imaging coordinates fails. This can also happen for combinations of skew lenses, namely, when the optical axis through the principal points is parallel to the transverse planes. This is the case when the intersection I between the image-sided focal plane of L_1 and the object-sided focal plane of L_2 intersects the optical axis through the principal points of the two lenses. The case of parallel confocal lenses is a special case of this situation: the intersection I between the relevant focal planes becomes a plane instead of a line, and this plane intersects the optical axis.

As mentioned above, the systems of lens-imaging coordinates are complementary. One way of looking at this is as follows. The image-sided Buchroeder coordinates are rotated relative to the object-sided ones. For this reason, the Buchroeder coordinates are well suited to problems involving a rotation between object and image space. Similarly, our lens-imaging coordinates are sheared relative to each other in the direction of the optical axis. Our lens-imaging coordinates are therefore particularly suited to understanding a shearing between object and image space.

We can use the ideas discussed in this paper to generalize the Scheimpflug principle [27]. Let us consider an object line with slope q, which intersects the optical axis at point z_o. Such a line

can be parametrized as $x = q(z - z_o)$, or equivalently $z = z_o + x/q$. Then the deflection angle θ formed by image line and the optical axis can be expressed by the equation

$$\cot\theta = \frac{z'(z_o + x/q, x) - z'(z_o, 0)}{x'(z_o + x/q, x) - x'(z_o, 0)} = \frac{1}{k_i} + \left(\frac{1}{q} - \frac{1}{k_o}\right)\frac{f}{f + z_o - P_z}. \tag{55}$$

If we define $1/q' \equiv \cot\theta$ (where, of course, q' is the slope of the image line), Eq. (55) can be rewritten in the more familiar form

$$\frac{1}{q'} - \frac{1}{k_i} = \left(\frac{1}{q} - \frac{1}{k_o}\right)\frac{f}{f + z_o - P_z}, \tag{56}$$

which is, in fact, an imaging equation for the slopes. It is obvious that the scaling factor on the right-hand side of Eq. (56) and consequently the image slope q' is object-position dependent. Note that the left-hand side of Eq. (56) equals the inverse of the image slope expressed in (u, w) coordinates and the expression in brackets on the right-hand side equals the inverse of the object slope expressed in the (u', w') coordinate system.

8. CONCLUSIONS

We present a simple and elegant description of imaging by a pair of lenses that do not share an optical-axis direction. We describe such a combination as a single lens in which the object and image spaces are sheared. We show how to construct the optical axis, the direction of the transverse planes on both sides, and all cardinal points. This construction is remarkably simple; it has the potential to find use for designing and understanding novel optical devices.

We stress that the optical axis in Buchroeder lens-imaging coordinates is different from that in ours. This is in contrast to the focal planes, the principal planes, and in fact all transverse planes, which are the same in both coordinates. Note that, even in the case of a single lens, any straight line through the principal point can serve as the optical axis in a set of lens-imaging coordinates.

In future, we intend to apply our lens-imaging coordinates to the study of ideal-lens transformation-optics devices [10], which was the reason for developing these coordinates in the first place.

Funding. Engineering and Physical Sciences Research Council (EPSRC) (EP/M010724/1).

Acknowledgment. Many thanks to Stephen Oxburgh for useful discussions.

REFERENCES

1. U. Leonhardt, "Optical conformal mapping," Science **312**, 1777–1780 (2006).
2. M. Šarbort and T. Tyc, "Spherical media and geodesic lenses in geometrical optics," J. Opt. **14**, 075705 (2012).
3. A. H. Layard, *Discoveries in the Ruins of Nineveh and Babylon* (G. P. Putnam, 1853), pp. 197–198.
4. M. Khorasaninejad, F. Aieta, P. Kanhaiya, M. A. Kats, P. Genevet, D. Rousso, and F. Capasso, "Achromatic metasurface lens at telecommunication wavelengths," Nano Lett. **15**, 5358–5362 (2015).
5. M. Khorasaninejad, W. T. Chen, R. C. Devlin, J. Oh, A. Y. Zhu, and F. Capasso, "Metalenses at visible wavelengths: diffraction-limited focusing and subwavelength resolution imaging," Science **352**, 1190–1194 (2016).
6. E. Arbabi, A. Arbabi, S. M. Kamali, Y. Horie, and A. Faraon, "Multiwavelength polarization-insensitive lenses based on dielectric metasurfaces with metamolecules," Optica **3**, 628–633 (2016).
7. W. T. Chen, A. Y. Zhu, V. Sanjeev, M. Khorasaninejad, Z. Shi, E. Lee, and F. Capasso, "A broadband achromatic metalens for focusing and imaging in the visible," Nat. Nanotechnol. **13**, 220–226 (2018).
8. J. S. Choi and J. C. Howell, "Paraxial ray optics cloaking," Opt. Express **22**, 29465–29478 (2014).
9. T. Tyc, S. Oxburgh, E. N. Cowie, G. J. Chaplain, G. Macauley, C. D. White, and J. Courtial, "Omnidirectional transformation-optics cloak made from lenses and glenses," J. Opt. Soc. Am. A **33**, 1032–1040 (2016).
10. J. Courtial, T. Tyc, J. Bělín, S. Oxburgh, G. Ferenczi, E. N. Cowie, and C. D. White, "Ray-optical transformation optics with ideal thin lenses makes omnidirectional lenses," Opt. Express **26**, 17872–17888 (2018).
11. W. J. Smith, *Modern Optical Engineering*, 3rd ed. (McGraw-Hill, 2000).
12. R. A. Buchroeder, "Tilted component optical systems," Ph.D. thesis (University of Arizona, 1976).
13. J. Bělín and J. Courtial, "Mathematica notebooks related to imaging with two skew ideal lenses," figshare (2018), https://doi.org/10.6084/m9.figshare.7195760.v1.
14. M. Born and E. Wolf, *Principles of Optics*, 7th ed. (Cambridge University, 1999), chap. 4.3.1.
15. G. J. Chaplain, G. Macauley, J. Bělín, T. Tyc, E. N. Cowie, and J. Courtial, "Ray optics of generalized lenses," J. Opt. Soc. Am. A **33**, 962–969 (2016).
16. C. Hahlweg, W. Zhao, and H. Rothe, "Fourier planes vs. Scheimpflug principle in microscopic and scatterometric devices," Proc. SPIE **8127**, 812708 (2011).
17. P. Gimenez-Benitez, J. C. Miñano, J. Blen, R. M. Arroyo, J. Chaves, O. Dross, M. Hernández, and W. Falicoff, "Simultaneous multiple surface optical design method in three dimensions," Opt. Eng. **43**, 1489–1503 (2004).
18. N. Yu, P. Genevet, M. A. Kats, F. Aieta, J.-P. Tetienne, F. Capasso, and Z. Gaburro, "Light propagation with phase discontinuities: generalized laws of reflection and refraction," Science **334**, 333–337 (2011).
19. X. Ni, A. V. Kildishev, and V. M. Shalaev, "Metasurface holograms for visible light," Nat. Commun. **4**, 2807 (2013).
20. N. Yu and F. Capasso, "Flat optics with designer metasurfaces," Nat. Mater. **13**, 139–150 (2014).
21. G. Zheng, H. Mühlenbernd, M. Kenney, G. Li, T. Zentgraf, and S. Zhang, "Metasurface holograms reaching 80% efficiency," Nat. Nanotechnol. **10**, 308–312 (2015).
22. L. Wang, S. Kruk, H. Tang, T. Li, I. Kravchenko, D. N. Neshev, and Y. S. Kivshar, "Grayscale transparent metasurface holograms," Optica **3**, 1504–1505 (2016).
23. P. Genevet, F. Capasso, F. Aieta, M. Khorasaninejad, and R. Devlin, "Recent advances in planar optics: from plasmonic to dielectric metasurfaces," Optica **4**, 139–152 (2017).
24. F. Aieta, M. A. Kats, P. Genevet, and F. Capasso, "Multiwavelength achromatic metasurfaces by dispersive phase compensation," Science **347**, 1342–1345 (2015).
25. M. Khorasaninejad, A. Ambrosio, P. Kanhaiya, and F. Capasso, "Broadband and chiral binary dielectric meta-holograms," Sci. Adv. **2**, e1501258 (2016).
26. H.-T. Chen, A. J. Taylor, and N. Yu, "A review of metasurfaces: physics and applications," Rep. Prog. Phys. **79**, 076401 (2016).
27. T. Scheimpflug, "Improved method and apparatus for the systematic alteration or distortion of plane pictures and images by means of lenses and mirrors for photography and for other purposes," GB patent 1196 (May 12, 1904).